

Version 00 as of November 14, 2019

Primary authors: Carlos Yero, Werner Boeglin, Mark Jones

To be submitted to PRL

Comment to ciero002@fiu.edu by xxx, yyy

DØ INTERNAL DOCUMENT – NOT FOR PUBLIC DISTRIBUTION

First Measurements of the D(e,e'p)n Cross Section at Very High Recoil Momenta and Large Q²

C. Yero and W.U. Boeglin

Florida International University, University Park, Florida 33199, USA

M.K. Jones

*Thomas Jefferson National Accelerator Facility,
Newport News, Virginia 23606, USA*

(for the Hall C Collaboration)

(Dated: November 14, 2019)

Abstract

First results of cross section measurements of the $^2H(e, e'p)n$ reaction at 4-momentum transfers ~~at neutron recoil angles of 35, 45 and 75 degrees.~~ $4 \leq Q^2 \leq 5 \text{ GeV}^2$ ~~and~~, neutron recoil momenta up to $p_r \sim 1.18 \text{ GeV}/c$ are presented. At the selected kinematics, Meson Exchange Currents (MEC) and Isobar Configurations (IC) are suppressed. Final State Interactions (FSI) have ~~also~~ been suppressed by choosing a kinematic region where the ~~in-plane neutron recoil angle (θ_{nq}) is between 35 and 45 degrees with respect to the 3-momentum transfer, \vec{q} .~~ In this region, the Plane Wave Impulse Approximation (PWIA) dominates ~~and provides the dominant cross section contribution~~ ~~the~~. Comparison to recent theoretical calculations show data to be sensitive to momentum distributions up to $p_r \sim 750 \text{ MeV}/c$.

Being the only two-nucleon bound system, (nucleon-nucleon) potential is expected to exhibit a repulsive core in which the interacting nucleon pair begins to overlap. The overlap distance scale, a region study the strong nuclear force at the subfermi level which is currently not well understood. At such small internucleon distances the NN correlations (SRC) observed in $A > 2$ nuclei

[1–4]. Short-range studies of the deuteron are also important in determining whether or to what extent ~~is~~ the description of nuclei in terms of nucleon/meson degrees of freedom valid before having to include explicit **degree of freedoms**, quark effects, which is an issue of fundamental importance in nuclear physics[5]. As of the present time, there are only a few nuclear physics experiments for which a transition between nucleonic to quark degrees of freedom been observed [6–8]. This Letter presents first results of $^2H(e, e'p)n$ in which kinematics were taken to the limit where a transition to non-nucleonic degrees of freedom is expected.

The most direct way to study the short range structure of the deuteron wavefunction (or equivalently, its high momentum components) is via the exclusive deuteron electro-disintegration reaction at very high neutron recoil (or missing) momenta ~~and within the Within the plane wave impulse approximation PWIA kinematics. In this approximation,~~ the virtual photon couples to the proton **subsequently** which is ejected from the nucleus without further interaction with the recoiling neutron, which carries a momentum equal in magnitude but opposite in direction to the initial state proton, $\vec{p}_r = -\vec{p}_{i,p}$. ~~This gives direct thus providing information on the momentum of the bound nucleon and its momentum distribution~~ since the scattered neutron momentum remains unchanged from its initial state.

In reality, the ejected particles un-

dergo subsequent interactions resulting in re-scattering between the proton and neutron (FSIs). Another possibility is that the photon may couple to the virtual meson being exchanged between the nucleons (MECs), or the photon may excite either nucleon in the deuteron into a resonance state (ICs) which decays back into the ground state nucleon causing futher re-scattering between the proton and neutron. Both MECs and ICs in addition to FSIs can significantly alter the recoiling neutron momentum thereby obscuring any possibility of directly accessing the deuteron momentum distributions.

Previous deuteron electro-disintegration experiments performed at Jefferson Lab (JLab) have helped constrain and quantify the contributions from FSIs, MECs and ICs on the $^2H(e, e'p)n$ cross-section and determine the kinematics at which they are either suppressed (MECs and ICs) or under control (FSIs). The first of these was performed in Hall A [9] at a relatively low momentum transfer of $Q^2 = 0.665 \text{ GeV}^2$ and neutron recoil momenta up to $p_r = 550 \text{ MeV}/c$ where it was shown that for $p_r > 300 \text{ MeV}/c$, FSIs, **dominate the cross section** MECs and ICs ~~played a significant role~~ and had to be included in Arenhövel's calculations [10–13] for a satisfactory agreement between theory and data.

The next experiment was performed in Hall B [14] using the CEBAF Large Accep-

tance Spectrometer (CLAS) which measured a wide variety of kinematic settings giving an overview of the $^2H(e, e'p)n$ reaction kinematics. This was the first experiment to probe the deuteron at high momentum transfers ($1.75 \leq Q^2 \leq 5.5 \text{ GeV}^2$) and presented angular distributions of cross-sections that confirmed the onset of the General Eikonal Approximation (GEA)[15, 16], which predicts a strong angular dependence of FSI with neutron recoil angles with a peak at $\theta_{nq} \sim 70^\circ$. The cross sections versus neutron recoil momenta up to $p_r \sim 2 \text{ GeV}/c$ were also presented, however, statistical limitations made it necessary to integrate over a wide angular range making it impossible to control contributions from FSI, MEC and IC

Finally, a third $^2H(e, e'p)n$ experiment was performed in Hall A [17] at ~~published~~ $Q^2 = 3.5 \pm 0.25 \text{ GeV}^2$ and recoil momenta up to $550 \text{ MeV}/c$. The angular distributions of the cross-section ratio ($R = \sigma_{exp}/\sigma_{PWIA}$) presented ~~verified~~ ~~confirmed~~ the strong anisotropy of FSIs with recoil angle θ_{nq} also observed in Hall B[14]. Most importantly, for recoil neutron momentum bins, $p_r = 0.4 \pm 0.02$ and $0.5 \pm 0.02 \text{ GeV}/c$, the ratio was found to be $R \sim 1$ for $35^\circ \leq \theta_{nq} \leq 45^\circ$ indicating a reduced sensitivity of the experimental cross-section to FSIs. This kinematic window allowed for the first time the extraction of momentum distributions for neutron recoil momenta up to

$p_r \sim 550 \text{ MeV}/c$.

The experiment presented on this Letter takes advantage of the kinematic window previously found in Hall A[17] and extends the $^2H(e, e'p)n$ cross section measurements to $Q^2 = 4.5 \pm 0.5 \text{ GeV}^2$ and neutron recoil momenta up to $1.18 \text{ GeV}/c$. At these kinematics, MECs and ICs are suppressed and FSIs are under control for neutron recoil angles between 35 and 45 degrees giving access to unprecedented high momentum components of the deuteron wavefunction.

This experiment was part of a group of four experiments that commissioned the new Hall C Super High Momentum Spectrometer (SHMS) as part of the 12 GeV upgrade at JLab. A 10.6005 GeV electron beam was incident on a 10 cm long liquid deuterium target (LD2). The scattered electron and knocked-out proton were detected in coincidence by the SHMS and High Momentum Spectrometer (HMS), respectively. The “missing” (undetected) neutron was reconstructed from momentum conservation laws. The beam currents delivered by the accelerator ranged between 40-60 μA due to frequent beam trips at higher currents and the beam was rastered over a $2 \times 2 \text{ mm}^2$ area to reduce the effects of localized boiling on the cryogenic targets (hydrogen and deuterium).

Both spectrometers at Hall C have similar standard detector packages, each with

1) four sets of hodoscope planes[18] (scintillator arrays) used for triggering, 2) a pair of drift chambers[19] used for tracking, 3) a calorimeter[20] used for e^-/π^- discrimination and 4) a gas Čerenkov [21, 22] used also for e^-/π^- separation. Due to the absence of significant background on this experiment and the low coincidence trigger rates ($\sim 1 - 3$ Hz) at the higher missing momentum settings, the use of additional particle identification (PID) was found to have little to no effect on the final cross section.

We measured three missing momentum settings: $p_r = 80, 580$ and 750 MeV/c. In the high missing momentum settings the spectrometer configuration was changed multiple times resulting in either the spectrometer angle or momentum not being exactly the same. As a result, two separate data sets were measured for the 580 MeV/c setting and three data sets for the 750 MeV/c setting. The spectrometer central settings are approximately as follows: the SHMS central angle and momentum settings were kept “fixed” at (~ 12.194 deg, 8.5342 GeV/c) and the HMS central angle and momentum settings were changed from (38.896 deg, 2.840 GeV/c) at the 80 MeV setting to $\sim(54.992$ deg, 2.1925 GeV/c) and $\sim(58.391$ deg, 2.0915 GeV/c) at the 580 and 750 MeV/c settings, respectively.

At these kinematics, the 3-momentum transfer is $|\vec{q}| \sim 2.88$ GeV/c which is more

than twice the highest neutron recoil momentum (p_r) measured on this experiment. As a result one can infer that most of the virtual photon momentum is transferred to the proton which scatters at angles relative to \vec{q} , $\theta_{pq} \sim 0$. This configuration is known as the “parallel-kinematics” and suppresses the process in which the neutron is struck while the detected proton is a spectator. FSIs are also expected to be largely reduced as compared to the “perpendicular-kinematics” in which the proton is detected almost perpendicular to \vec{q} based on a calculation by Arenhövel on Table 1 of Ref.[5].

In addition to deuteron kinematics, $^1H(e, e'p)$ elastic data was also taken at kinematics close to the deuteron 80 MeV setting for cross-checks with the spectrometer acceptance model as well as for normalization purposes using the Hall C Monte Carlo simulation program, SIMC. Additional $^1H(e, e'p)$ data were also taken at three other kinematic settings that covered the entire SHMS momentum acceptance range and were used for spectrometer optics optimization, momentum calibration and determination of the spectrometer offsets and kinematic uncertainties[23, 24].

The event selection criteria was done exactly the same for the hydrogen and deuteron data. The criteria were determined by making 1) standard cuts on the spectrometer momen-

Why not give the range of angles

I would not use this terminology. Stay with the neutron recoil angle or use $x > 1$ regions

Are you sure that you know that many digits?

you cannot eliminate the tail, in fact you should not.

tum fraction (δ) to select a region in which the reconstruction optics is well known, 2) an ~~HMS~~ collimator cut to restrict the spectrometer solid angle acceptance to events that only directly passed through the collimator and not by re-scattering from the collimator edges, 3) a missing energy cut (peak ~ 2.22 MeV for the $d(e,e;p)$ deuteron) to select true $e'p$ coincidences and not events from the radiative tail, 4) a coincidence time cut to select true coincidence events and not accidentals, 5) a PID cut on the SHMS calorimeter to select electrons and not other sources of background, mostly pions and 6) a z -vertex difference cut between the HMS and SHMS z reaction vertex difference to select events that truly originated from the same reaction vertex at the target.

a cut on the reconstructed HMS and SHMS reaction vertices

The experimental data yield was normalized by the total charge and corrected for tracking efficiencies, total live time, proton absorption[25] and target boiling factors[26]. For $^1H(e, e'p)$, the corrected data yield was compared to SIMC using P. Bosted's proton form factor parametrization[27] to check the spectrometer acceptance model. The data to SIMC yield ratio integrated over invariant mass W was determined to be unity, so there was no need to include an overall hydrogen normalization factor. For the $^2H(e, e'p)n$ data, the measured cross sections were compared to the model cross sections (incorporated as a SIMC subroutine) from

calculations by J.M. Laget using the Paris potential[28]. Variations of up to $\sim 20\%$ for recoil momenta up to ~ 250 MeV/c were observed which are typical for this setting using the Paris potential. The 80 MeV data was also checked for reproducibility against the Hall A data (See Fig. 2). This agreement gives us confidence on the measurements made at higher missing momentum settings for which no previous data exists.

The systematic uncertainties on the measured cross sections were determined from normalization[29] and kinematic uncertainties. The individual contributions from normalization uncertainties were determined to be: tracking efficiencies (0.40%-HMS, 0.59%-SHMS), target boiling (0.39%), total live time (3.0%) and total charge (2.0%) for an overall normalization uncertainty added in quadrature of 3.7%.

The kinematic uncertainties were determined point-to-point in (θ_{nq}, p_r) bins for each data set independently, and added in quadrature for overlapping p_r bins of different data sets. For $\theta_{nq} = 35, 45$ and 75 deg (presented on this Letter) the overall kinematic uncertainty varied up to 6.5% for $p_r \leq 1.01$ GeV/c. The overall systematic uncertainty in the cross section was determined by the quadrature sum of the normalization and kinematic uncertainties. This results was then added in quadrature to the statiscal uncertainty(25-

This is not clear what is W does this refer to single arm ?

For each bin in (θ_{nq}, p_r) the averaged $d(e,e'p)n$ kinematic has been calculated. The ratio between the calculated cross section for this averaged kinematics and the averaged cross section for this bin has been determined and used to compare theoretical models to the experimental cross sections. The calculations were based on the Laget model including FSI (ref 28)

30% on average) to obtain the final uncertainty in the cross section.

The data was radiatively corrected for each bin in (θ_{nq}, p_r) by multiplying measured cross sections to the ratio of the SIMC yield without and with radiative effects. Bin-centering corrections were also applied by multiplying the radiative corrected cross sections to the ratio of theoretical cross sections (external to SIMC) to the average cross sections calculated from SIMC. The theoretical calculations used in the bin-centering corrections were done by J.M. Laget using the Paris potential[28] including FSI

Both experimental and theoretical reduced cross sections were extracted from the measured (or model) cross sections for each data set independently and were averaged for overlapping bins in p_r . The reduced cross sections are defined as follows:

$$\sigma_{red} \equiv \frac{\sigma_{exp(th)}}{K f_{rec} \sigma_{cc1}} \quad (1)$$

where $\sigma_{exp(th)}$ is the 5-fold experimental (or theoretical) differential cross section $\frac{d^5\sigma}{d\omega d\Omega_e d\Omega_p}$, K is a kinematical factor, f_{rec} is the recoil factor that arises from the integration over missing energy and σ_{cc1} is the de Forest[30] electron-proton offshell cross section calculated using P. Bosted's form factor parametrization [27]. Only within the PWIA, σ_{red} corresponds to the experimental (or theoretical) reduced cross section $n(p_r)$.

I am not convinced that this level of detail is necessary here

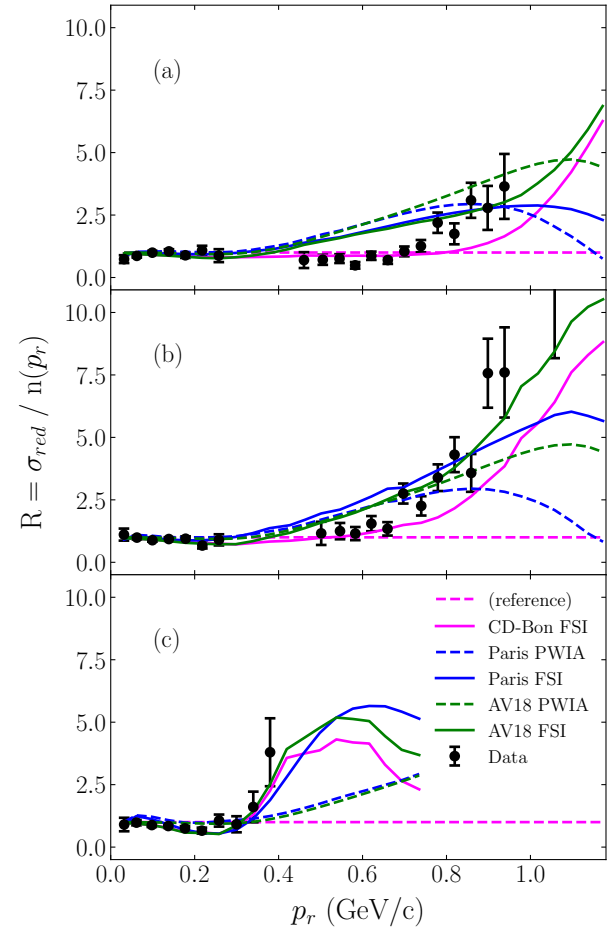


FIG. 1. The ratio $R(p_r) = \sigma_{red}/n(p_r)$ is shown in (a)-(c) for $\theta_{nq} = 35^\circ, 45^\circ$ and 75° , respectively, each with a bin width of $\pm 5^\circ$. The dashed reference (magenta) line refers to CD-Bonn momentum distribution ($n(p_r)$) by which the data and all models are divided.

most of the kinematical dependencies that arise from the cross section have been factored out by σ_{cc1} , leaving only a dependency on p_r .

To quantify by how much and to what extent the data agrees with theory, the ratio of the experimental (or theoretical) reduced

cross sections (σ_{red}) relative to the deuteron momentum distributions ($n(p_r)$) using the As a reference we selected the deuteron charge dependent Bonn (CD-Bonn)[31] momentum distribution calculated using the CD-Bonn potential.

Theoretical calculations for the CD-Bonn and Ar-

gonne v_{18} (AV18)[32] potentials were per-

Reference: M.M.Sargsian, PRC 82, 2010, 014612

formed by M. Sargsian and those for the Paris

Reference: J.M.Laget PLB 609, 2004, 49

potential[28] were done by J.M. Laget. For

$p_r \lesssim 300$ MeV/c, the data is in good agree-

ment with all models for the neutron recoil angles shown in Fig. 1. For $p_r \gtrsim 300$, at

recoil angles $\theta_{nq} = 35^\circ \pm 5^\circ$ [Fig. 1(a)], the

calculations using the potential

data is best described by the CD-Bonn curves

which exhibiting a reduced sensitivity to FSIs

and an enhanced sensitivity to the momen-

tum distribution with a ratio $R \sim 1$ for recoil

momenta up to ~ 800 MeV/c before being

overwhelmed by FSIs. The data, however, is

sensitive to the momentum distributions only

up to $p_r \sim 750$ MeV/c before transitioning to

other theoretical curves with a maximal ratio

of $R \sim 3$ at $p_r \sim 940$ MeV/c due to statistical

limitations. For recoil angles $\theta_{nq} = 45^\circ \pm 5^\circ$

[Fig. 1(b)], both the data and CD-Bonn

curves show sensitivities to momentum distri-

butions up to $p_r \sim 580$ MeV/c. At $p_r > 580$

MeV/c, FSIs become increasingly important

for CD-Bonn, whereas the data shows a simi-

lar behaviour as in Fig. 1(a) with an early

rise in the ratio than predicted by the CD-

Bonn FSI model. For $\theta_{nq} = 75^\circ \pm 5^\circ$ [Fig.

1(c)], the onset of GEA is observed beyond

$p_r \sim 300$ MeV/c, with a strong angular dependence of the reduced cross sections on FSIs predicted by all models and verified by data which was statistically limited at larger recoil angles.

Figure 2 shows the extracted experimen-

tal and theoretical reduced cross sections as a

function of neutron recoil momentum p_r for

three angular settings at $4 \leq Q^2 \leq 5$ GeV².

The data is compared to the results from the

previous Hall A experiment[17] at a $Q^2 = 3.5$

GeV². The overlay of the Hall A data (cyan)

in Fig. 2 provides a continuity to the data

from this experiment in the transition from

low (80 MeV/c) to high (580, 750) MeV/c

missing momentum settings in which there

was no data. There is also an overall good

agreement between the two experiments in

the regions in which they overlap in p_r .

At larger neutron recoil angles of $\theta_{nq} \sim$

75° [Fig. 2(c)], the data follows the CD-

Bonn PWIA (momentum distributions) up

to $p_r \sim 100$ MeV/c, and at $p_r \gtrsim 300$ MeV/c,

the FSIs become the dominant process and

exhibit a smaller falloff with p_r which ob-

scures any possibility of extracting the mo-

mentum distributions. This behaviour of FSI

with larger recoil angles was predicted by

the GEA[15, 16] and was verified in previous

experiments[14, 17]. This experiment kine-

matics moves away from larger recoil angles

and focuses on forward angles at $\theta_{nq} \sim 40^\circ$

where the momentum distributions become accessible. As a result, our data at larger recoil angles is statistically limited.

For recoil angles at $\theta_{nq} = 35^\circ$ and 45° shown in Figs. 2(a) and 2(b), all models predict similar behaviour of the momentum distribution for recoil momenta up to $p_r \sim 300$ MeV/c which the data verifies. At larger p_r , however, the momentum distributions become increasingly sensitive to the different NN potentials, mainly a difference between

the CD-Bonn and either the Paris or AV18 is observed.

In Fig. 2(a) for example, the data is clearly sensitive to the CD-Bonn momentum distributions between recoil momenta of $300 \lesssim p_r \lesssim 750$ MeV/c before transitioning to the Paris/AV18 potentials which is a behaviour that is not well described by any of the models. For recoil angles in Fig. 2(b), a similar behaviour can be observed, as the data is sensitive to the CD-Bonn momentum dis-

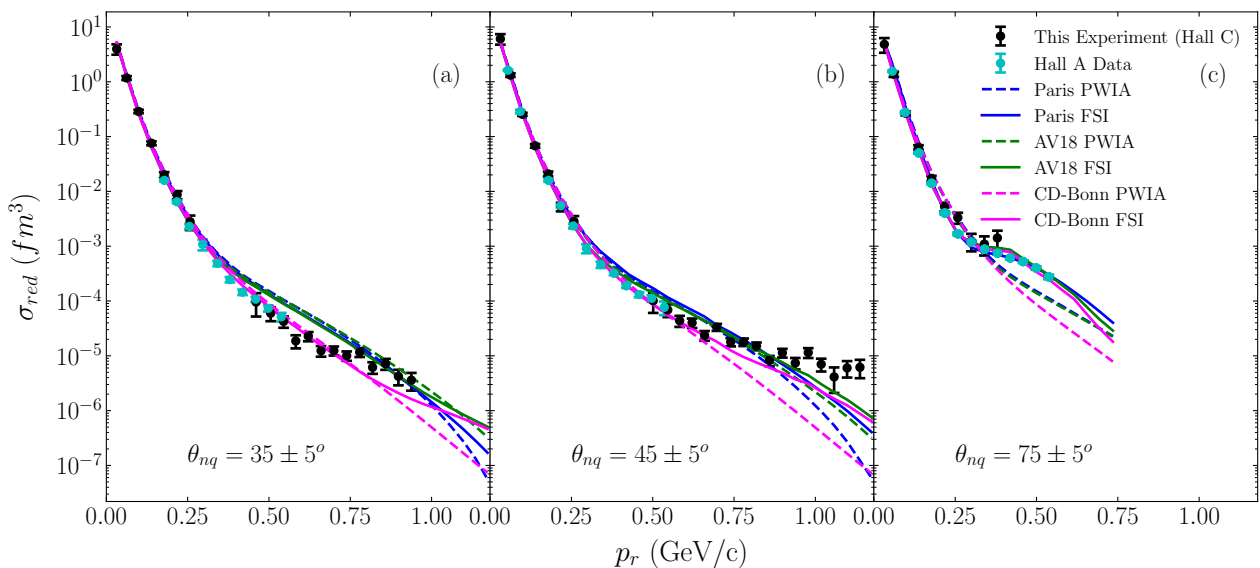


FIG. 2. The reduced cross sections $\sigma_{red}(p_r)$ as a function of neutron recoil momentum p_r are shown in (a)-(c) for recoil angles $\theta_{nq} = 35^\circ, 45^\circ$ and 75° , respectively, with a bin width of $\pm 5^\circ$. The data is compared to the previous Hall A experiment (cyan) results[17] as well as the Paris(blue), AV18(green) and CD-Bonn(magenta) theoretical reduced cross sections.

tributions but only up to $p_r \sim 580$ MeV/c as FSIs start to dominate at lower p_r as op-

posed to Fig. 2(a). For $p_r > 580$ MeV/c, the data again exhibits a behaviour at the high momentum tails which either the CD-Bonn, Paris or AV18 potentials are unable to describe.

This commissioning experiment extended the previous Hall A cross section measurements on the $^2H(e, e'p)n$ reaction to unprecedented large Q^2 and very high neutron recoil momenta at kinematics that enhances the high momentum components of the deuteron wavefunctions. The experimental reduced cross sections were extracted and found to be best described by the CD-Bonn potential with sensitivity to the CD-Bonn momentum distributions up to $p_r \sim 580$ and 750 MeV/c for $\theta_{nq} \sim 45^\circ$ and 35° , respectively before the data transitioning to other theoretical models, which is a behavior that was not predicted by any of the models.

Given that this experiment ran for only 6 out of the 42 days (21 PAC days assuming 100% beam efficiency) of beam time and 3 out of the 8 kinematic settings approved in the original proposal[33], we conclude that additional beam time is required to measure the full kinematic coverage as the results presented on this Letter (although very interesting) do not have the necessary statistics and the required number of high missing momentum settings to make a definitive argument about the underlying physics observed.

We acknowledge the outstanding support of the staff of the Accelerator and Physics Divisions at Jefferson Lab as well as the entire Hall C staff, technicians, graduate students and users who took shifts or contributed to the equipment for the Hall C upgrade making all four commissioning experiments possible.

-
- [1] K. S. Egiyan *et al.* (CLAS Collaboration), Observation of nuclear scaling in the $A(e, e')$ reaction at $x_B > 1$, *Phys. Rev. C* **68**, 014313 (2003).
 - [2] K. S. Egiyan *et al.* (CLAS Collaboration), Measurement of two- and three-nucleon short-range correlation probabilities in nuclei, *Phys. Rev. Lett.* **96**, 082501 (2006).
 - [3] R. Shneor *et al.* (Jefferson Lab Hall A Collaboration), Investigation of proton-proton short-range correlations via the $^{12}\text{C}(e, e'pp)$ reaction, *Phys. Rev. Lett.* **99**, 072501 (2007).
 - [4] N. Fomin, D. Higinbotham, M. Sargsian, and P. Solvignon, New results on short-range correlations in nuclei, *Annual Review of Nuclear and Particle Science* **67**, 129159 (2017).
 - [5] P. Ulmer *et al.*, Short-Distance Structure of the Deuteron and Reaction Dynamics in $^2\text{H}(e, e'p)n$, https://www.jlab.org/exp_prog/proposals/01/PR01-020.pdf

- (2001), *Jefferson Lab Proposal E01-020*.
- [6] C. Bochna *et al.*, Measurements of deuteron photodisintegration up to 4.0 gev, *Phys. Rev. Lett.* **81**, 4576 (1998).
- [7] E. C. Schulte *et al.*, Measurement of the high energy two-body deuteron photodisintegration differential cross section, *Phys. Rev. Lett.* **87**, 102302 (2001).
- [8] E. C. Schulte *et al.*, High energy angular distribution measurements of the exclusive deuteron photodisintegration reaction, *Phys. Rev. C* **66**, 042201 (2002).
- [9] P. E. Ulmer *et al.*, $^2\text{H}(e, e' p)n$ reaction at high recoil momenta, *Phys. Rev. Lett.* **89**, 062301 (2002).
- [10] H. Arenhövel, W. Leidemann, and E. L. Tomusiak, Inclusive deuteron electrodisintegration with polarized electrons and a polarized target, *Phys. Rev. C* **43**, 1022 (1991).
- [11] H. Arenhövel, W. Leidemann, and E. L. Tomusiak, Exclusive deuteron electrodisintegration with polarized electrons and a polarized target, *Phys. Rev. C* **46**, 455 (1992).
- [12] H. Arenhövel, W. Leidemann, and E. L. Tomusiak, Nucleon polarization in exclusive deuteron electrodisintegration with polarized electrons and a polarized target, *Phys. Rev. C* **52**, 1232 (1995).
- [13] H. Arenhövel, F. Ritz, H. Göller, and T. Wilbois, Consistent treatment of relativistic effects in electrodisintegration of the deuteron, *Phys. Rev. C* **55**, 2214 (1997).
- [14] K. S. Egiyan *et al.* (CLAS Collaboration), Experimental study of exclusive $^2\text{H}(e, e' p)n$ reaction mechanisms at high Q^2 , *Phys. Rev. Lett.* **98**, 262502 (2007).
- [15] M. M. Sargsian, Selected Topics in High Energy Semi-Exclusive Electro-Nuclear Reactions, *International Journal of Modern Physics E* **10**, 405457 (2001).
- [16] L. L. Frankfurt, M. M. Sargsian, and M. I. Strikman, Feynman graphs and generalized eikonal approach to high energy knock-out processes, *Phys. Rev. C* **56**, 1124 (1997).
- [17] W. U. Boeglin *et al.* (For the Hall A Collaboration), Probing the high momentum component of the deuteron at high Q^2 , *Phys. Rev. Lett.* **107**, 262501 (2011).
- [18] G. Niculescu, I. Niculescu, M. Burton, D. Coquelin, K. Nisson, and T. Jarell, Shms hodoscope scintillator detectors, https://hallcweb.jlab.org/document/howtos/shms_scintillator_hodoscope.pdf.
- [19] M. Christy, P. Monaghan, N. Kalantarians, D. Biswas, and M. Long, Shms drift chambers, https://hallcweb.jlab.org/document/howtos/shms_drift_chambers.pdf.
- [20] H. Mkrtchyan *et al.*, The lead-glass electromagnetic calorimeters for the magnetic

- spectrometers in hall c at jefferson lab, *Nuclear Instruments and Methods in Physics Research Section A: Accelerators, Spectrometers, Detectors and Associated Equipment* **719**, 85100 (2013).
- [21] W. Li, *Heavy Gas Cherenkov Detector Construction for Hall C at Thomas Jefferson National Accelerator Facility*, Master's thesis, University of Regina (2012).
- [22] D. Day, Preliminary design of the shms noble cerenkov detector, <https://hallcweb.jlab.org/DocDB/0009/000933/001/shms-cerv6.pdf>.
- [23] C. Yero, Update on spectrometer offsets determination using h(e,e'p) elastics (2019), https://hallcweb.jlab.org/DocDB/0010/001036/002/HC_SoftwareMeeting_0ct03_2019_pdf.pdf.
- [24] C. Yero, Optics optimization for the d(e,e'p)n experiment [e12-10-003] (2019), https://hallcweb.jlab.org/DocDB/0010/001033/001/d2_optim.pdf.
- [25] C. Yero, Proton absorption (2019), https://hallcweb.jlab.org/DocDB/0010/001020/002/ProtonAbsorption_slides.pdf.
- [26] C. Yero, Hms target boiling studies (2019), https://hallcweb.jlab.org/DocDB/0010/001023/003/TargetBoiling_v2.pdf.
- [27] P. E. Bosted, Empirical fit to the nucleon electromagnetic form factors, *Phys. Rev. C* **51**, 409 (1995).
- [28] M. Lacombe, B. Loiseau, J. M. Richard, R. V. Mau, J. Côté, P. Pirès, and R. de Tourreil, Parametrization of the paris $n-n$ potential, *Phys. Rev. C* **21**, 861 (1980).
- [29] Conservative estimates on the systematic uncertainties of the total live and charge were made. Determination of systematics on these quantities is a work in progress. (Private communication with D. Mack).
- [30] T. D. Forest, Off-shell electron-nucleon cross sections: The impulse approximation, *Nuclear Physics A* **392**, 232 (1983).
- [31] R. Machleidt, High-precision, charge-dependent bonn nucleon-nucleon potential, *Phys. Rev. C* **63**, 024001 (2001).
- [32] R. B. Wiringa, V. G. J. Stoks, and R. Schiavilla, Accurate nucleon-nucleon potential with charge-independence breaking, *Phys. Rev. C* **51**, 38 (1995).
- [33] W. U. Boeglin *et al.*, Deuteron Electro-Disintegration at Very High Missing Momenta, https://www.jlab.org/exp_prog/proposals/10/PR12-10-003.pdf.

